Chapter 2. Survey of Previous Research in Charged Particle Dynamics, Droplets in Electric Fields, and Electrospray Ionization

Portions adapted from Grimm, R. L.; Beauchamp, J. L. *J. Phys. Chem. B* **2005**, *109*, 824 and Grimm, R. L.; Beauchamp, J. L. *Anal. Chem.* **2002**, *74*, 6291.

2.1. Introduction

This thesis explores the mechanisms and processes that occur during electrospray ionization as well as explores and develops new applications of field-induced droplet ionization mass spectrometry. Both electrospray and field-induced droplet ionization rely on creating electrical pressure within droplets and liquids. Sufficient electrical pressure drives instabilities and jetting both from charged and neutral droplets as well as liquids flowing from a capillary needle. Within droplets, instability and jetting may be the result of a strong applied electric field, sufficient net charge, or a combination of charge and applied field. The jets that form during these instabilities consist of charged progeny droplets that are a suitable source of desolvated ions for mass analysis.

This chapter reviews the history of electrospray ionization and the subsequent interest in charged droplet instabilities. Although much of the research occurred concurrently, electrospray, evaporation and discharge of highly charged droplets, and electric field-induced droplet ionization are separated for clarity. Section 2.2 presents a historical perspective of electrospray ionization from early experiments with blood through John Fenn's 2002 Nobel prize in chemistry. Understanding the dynamics of charged droplets is paramount to knowing how charged droplets produced by electrospray ultimately yield desolvated, gas-phase ions. Section 2.3 summarizes 120 years of charged droplet research from Lord Rayleigh's initial theories to recent work performed in the Beauchamp group.

Field-induced droplet ionization mass spectrometry (FIDI-MS) fundamentally depends on the behavior and response of a droplet to the application of an external electric field. In FIDI-MS an applied electric field elongates a neutral or lightly charged droplet parallel to the field, ejecting opposite jets of positively and negatively charged progeny droplets. These progeny droplets are directed into the atmospheric sampling capillary inlet of a mass spectrometer where dissolved analytes are mass analyzed. The behavior of neutral droplets in high electric fields is therefore critical to understanding FIDI. A history of the experiments and theoretical investigations on the topic are presented in section 2.4. Finally, section 2.5 discusses outstanding issues and avenues of future research related to charged droplet instability and field-induced droplet ionization.

2.2. A brief history of electrospray ionization

The phenomenon of electrospray was investigated long before it was applied to the study of gas phase ions transferred from solution. In 1750, French clergyman and physicist Jean-Antoine (Abbé) Nollet reported the earliest known reference to electrospray, over two hundred years before the term was coined. He demonstrated that water flowing from a vessel would aerosolize when the vessel was electrified and placed near electrical ground. He also observed that "a person, electrified by connection to a high-voltage generator, would not bleed normally if he were to cut himself; blood would spray from the wound."[1] Roughly one hundred years later, Lord Kelvin designed an apparatus consisting of two liquid nozzles connected to opposite collection reservoirs. Small statistical differences in charging between water dripping from the nozzles quickly led to kilovolt differences and electrosprays at the nozzles.[2]

In the early twentieth century, refined experimental techniques allowed for a more rigorous understanding of electrostatics and electrodynamics. John Zeleny classified the formation of ethanol electrosprays through photographs reprinted in Figure 2.1.[3] The sprays characterized in Zeleny's work are structurally similar to those employed for mass spectrometry today in which liquid is drawn into a conical shape before breaking into a fine mist of droplets. This work was followed by rigorous studies of the field-dependent deformation of soap films over cylindrical tubes by Wilson and Taylor. The conical shape of these films resembled Zeleny's observations of ethanol and indeed has come to be termed the Taylor cone based on later theoretical work by G. I. Taylor.[4,5]

By the middle of the twentieth century, electrospray had become a popular painting technique. Reports by Hines,[6] Tilney and Peabody,[7] and several patents demonstrate the ease with which paint is atomized and applied to vehicles, housewares, and various metal goods. However, it was not until 1968 that electrospray was introduced as a scientific tool. Dole and coworkers transferred high molecular weight polystyrene ions into the gas phase from a benzene/acetone solution.[8] They introduced the combination of electrospray and nozzle skimmer/pumping systems similar to those employed today to transfer the charged species from atmospheric pressure into the vacuum system for analysis. Although a revolutionary technique, Dole did little to develop electrospray into a rigorous experimental methodology.

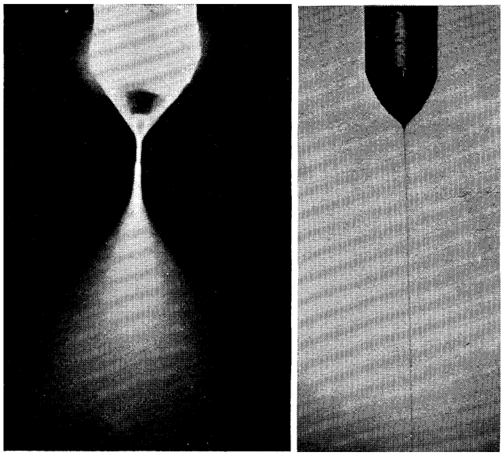

Figure 2.1. Early photographs of ethanol electrosprays. Reprinted Figure 5 and 7 with permission from Zeleny, J. *Phys. Rev.* **1917**, *10*, 1.[3] Copyright 1917 by the American Physical Society.

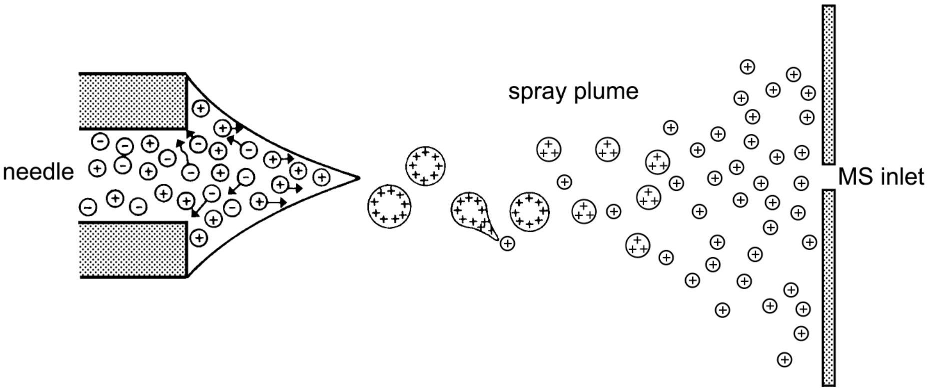

Figure 2.2. Electrospray ionization-mass spectrometry schematic. A high voltage power supply (not shown) establishes an electric field between a solution-filled capillary needle and the mass spectrometer inlet. As the liquid is pushed through the capillary, ion migration draws the liquid to a tip that emits a fine spray of charged droplets. These droplets are directed to an atmospheric-sampling inlet of a mass spectrometer for analysis.

In the 1980's, Fenn and coworkers presented a series of papers that permanently established electrospray as a tool to introduce dissolved analytes into the gas phase for mass analysis. Figure 2.2 shows a schematic cartoon of the electrospray ionization arrangement for mass spectrometry. Electrospray generates charged droplets that are directed towards a capillary sampling inlet of a mass spectrometer for analysis of the dissolved species in the sprayed solution. Their work attracted significant attention through spraying compounds of ubiquitous scientific interest including low molecular weight cationic clusters,[9] negative ions,[10] polyethylene glycol,[11] and several biomolecules.[12] They noted that electrospray imparts multiple charges to large biomolecules and polymers thus lowering the m/z value allowing biomolecule analysis on mass spectrometers having only a modest m/z range. ESI-MS has become a popular tool for studying noncovalent interactions and characterizing biomolecules. Cole reviews the present state and the diverse applications of electrospray ionization.[13]

2.3. Investigations of the behavior of highly charged droplets

The application of electrospray to mass spectrometry by Fenn and coworkers and its subsequent popularity renewed an interest in the process by which charged droplets yield desolvated, gas-phase ions. Because ESI generates charged droplets that ultimately produce gas-phase ions, understanding the processes that govern charged droplet breakup and evaporation is critical for understanding and refining ESI as well as its application to mass spectrometry.

2.3.1. Rayleigh's original conjectures regarding charged droplets

In 1882, Lord Rayleigh first considered the electrical pressure resulting from excess charge q on a droplet of spherical radius r and surface tension σ. His theory predicts that the natural quadrupolar oscillation of a droplet in a field-free environment becomes unstable when q exceeds the limit q_R, now known as the "Rayleigh limit", defined in equation (2.1).

$$q_\mathrm{R} = 8\pi\varepsilon^{1/2}\sigma^{1/2}r^{3/2} \tag{2.1}$$

The limit is reached either by evaporation or by application of charge in excess of q_R. At $q \geq q_\mathrm{R}$, Rayleigh postulated that the droplet would throw out liquid in fine jets.[14] This event is referred to in the literature as Rayleigh discharge[15,16] or Coulomb fission.[17] Despite a rigorous prediction of when the event occurs, Rayleigh's analysis does little to describe the dynamics of the discharge event.

2.3.2. Modern research on Rayleigh discharge phenomena

Recent articles by Cole[18] and by Kebarle and Peschke[19] summarize the research performed to elucidate the dynamics not described by Rayleigh's analysis. Figure 2.3 presents a cartoon summary of the "lifetime" of a charged droplet. In the consensus view, charged, micrometer-sized droplets eject numerous progeny droplets having a diameter roughly one-tenth that of the parent. Other experiments and models such as the ion desorption model and the charge residue model address phenomena involving smaller droplets in the nanometer regime not considered in this thesis. Ultimately the result of ion desorption or the charge residue mechanism is a desolvated ion, or in some cases an ion-bound water cluster.[20]

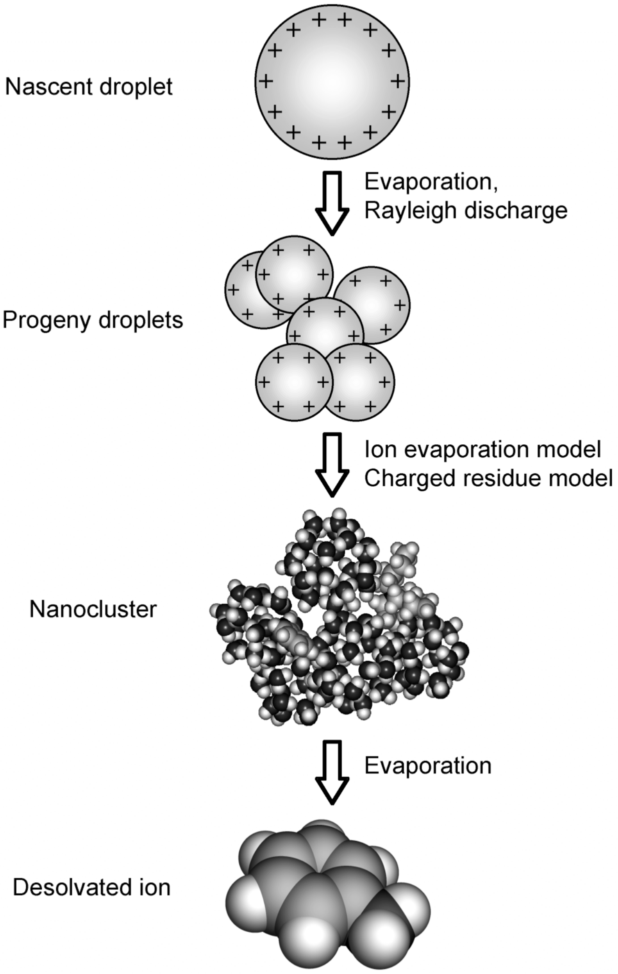

Figure 2.3. Cartoon depiction of the process by which a charged, analyte-containing droplet yields a desolvated, gas-phase ion. This thesis presents research into the Rayleigh discharge phenomenon shown in the first stage of charged droplet dynamics.

Table 2.1 summarizes the conclusions of Rayleigh discharge experiments found in the literature. This list is not inclusive, but rather shows the breadth and scope of the studies and their conclusions. Charged droplets generally undergo Rayleigh discharge while they are at 70-120% of their Rayleigh limit of charge. For instance, Taflin and co-workers found discharge occurring below 90% the Rayleigh limit with charge loss ranging from 10 to 18%, and 1-2% mass loss in dodecaonol, hexadecane, heptadecane, dibromooctane, and bromodecane.[21]

High speed photography by Gomez and Tang support the prevailing theories of Rayleigh discharge. Figure 2.4 shows a charged droplet undergoing jetting in an event attributed to Rayleigh discharge. In this event, it is clear that the parent is elongating and emitting a series of fine progeny droplets. Although they did not measure the charge lost during Rayleigh discharge, they noted the occurrence at ~60 to 80% the Rayleigh limit, and the photograph supports other experimental findings of little mass loss.[22]

More recently, Duft and co-workers explored Rayleigh discharge through accurate measurements of the quadrupolar oscillations in a droplet suspended in an alternating current electric field. Through a calculation of the Coloumb energy and surface energy of a droplet, they determined that ethylene glycol undergoes discharge at 100% q_R without reliance on the bulk surface tension parameter σ to determine q_R.[23] Recent studies in our laboratory focused on the more common electrospray solvents water, methanol, and acetonitrile. This work was performed in a mobility cell with an axial, linear electric field. Thus no field counteracts radial drift. Droplets are measured in a small measurement volume and the electric field reverses following measurement

Author(s)	Solvent	Location	Droplet Diam. (μm)	% q/q_R at Rayleigh Discharge	Percent Mass Lost	Percent Charge Lost
Li, Tu, and Ray, 2005[24]	diethyl phthalate	balance	5-25	96	2.3	21
	diethylene glycol			100	< 0.3	38
	triethylene glycol			100	< 0.3	41
	hexadecane			97	1.5	15
Duft et al., 2003[25]	ethylene glycol	balance	48	100	0.3	33
Duft et al., 2002[23]	ethylene glycol	balance	3-25	> 95	n/a	~25
Smith, Flagan, and Beauchamp, 2002[15]	water	IMS	10-60	100	n/a	20-40
	methanol			120		15-20
	acetonitrile			100		15-20
Feng et al., 2001[26]	methanol	balance	20-42	~ 100	n/a	80
Widmann et al., 1997[27]	50 BTD, 50 IDD	balance	25-30	3	24	21
	50 BTD, 50 IDD		17-28	3	75	74
	hexanediol diacrylate		22	64	n/a	n/a
Gomez, Tang, 1994[22]	heptane	ESI plume	32-80	60-80	n/a	n/a
Richardson et al., 1989[28]	*n*-octanol	balance	1-10	102	2.3	15
	sulfuric acid		1-10	84	< 0.1	49
Taflin, Ward, and Davis, 1989[21]	bromododecane	balance	44	72	n/a	12
	dibromooctane		26-40	86	1.8	16
	dibutyl phthalate		20	75	n/a	n/a
	docecanol		36-38	85	2	15
	hexadecane		28-64	73	1.6	17
	heptadecane		28-36	79	1.6	12
Roulleau et al., 1972[29]	water	balance	50-200	~100	n/a	n/a
Schweizer et al.,1971[30]	*n*-octanol	balance	15-40	~100	5	23
Berg et al., 1970[31]	balance	balance	30-250	25-100	n/a	n/a
Ataman et al., 1969[32]	*n*-octanol	balance	30-60	~100	n/a	n/a
Doyle, et al., 1964[33]	n/a	balance	60-200	n/a	n/a	30

Table 2.1. Survey of Rayleigh discharge studies from the literature. Abbreviations: BTD: 1-bromotetradecane, IDD: 1-iodododecane, IMS: ion mobility cell, balance: electrodynamic balance, ESI: electrospray ionization, n/a: not available. Superscripts refer to the references at the end of this chapter.

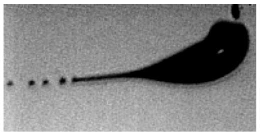

Figure 2.4. Instability and jetting from a charged heptane droplet within an electrospray plume. Reprinted with permission from Gomez, A.; Tang, K. *Phys. Fluids* **1994**, *6*, 404.[22] Copyright 1994, American Institute of Physics.

allowing multiple characterizations and the development of a time profile of droplet size and charge. That droplets are repeatedly characterized in a small measurement volume before and after Rayleigh discharge suggests a "soft" event in which little, if any, momentum is imparted to the parent droplet. This work also suggests a solvent dependence on the charge loss and the percent Rayleigh limit at discharge.[2,15]

2.4. Droplet instabilities driven by an applied electric field

Concurrent with investigations into the electrospray phenomenon, investigators considered the behavior of strong electric fields on *neutral* water droplets. In this case the applied electric field drives droplet instability rather than the charge repulsion due to a net surface charge. Early researchers saw meteorological implications and sought to understand how fields within clouds would affect rain and aerosol drops. In a classic 1931 experiment, Macky dropped ~1 to 5 mm diameter water droplets through a strong electric field with the apparatus shown in Figure 2.5A. Here a voltage difference between plates (i) and (ii) defines a high electric field. Water droplets are produced from reservoir (iii) through a stopcock (v) and field-free region (iv).

Macky observed that strong electric fields caused droplets to elongate into spheroids prolate to the electric field. At a critical field strength E_c^0, droplets developed instabilities resulting in the formation of two symmetrical fine filaments from opposing sides of the droplet. Figure 2.5B shows this elongation and instability in photographs of 5 mm diameter water droplets exposed to a 8250 V cm^{-1} electric field.

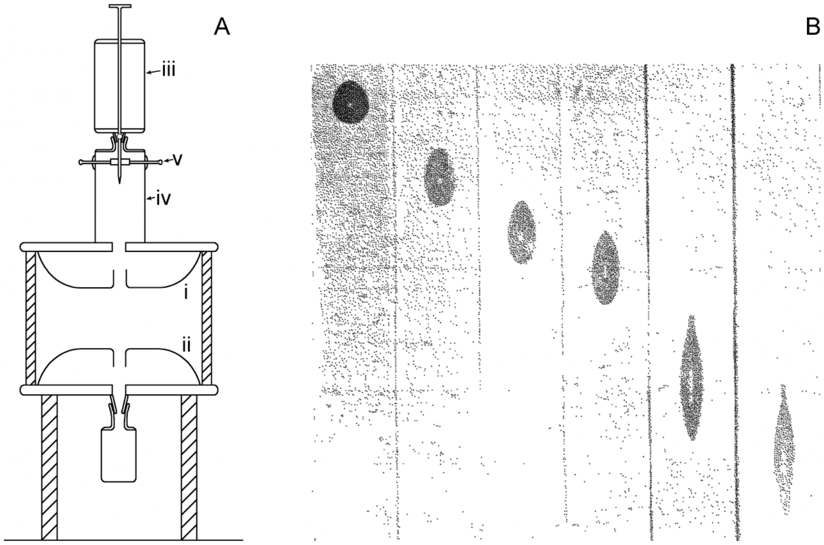

Figure 2.5. Early experimental apparatus (A) and photographs of droplets in strong electric fields (B). Adapted with permission from Macky, W.A. *Proc. Roy. Soc. A* **1931**, *133*, 565. Copyright 1931, the Royal Society.[34]

Macky[34] and other researchers[35,36] noted the relationship between the critical electric field necessary to induce an instability and jetting in neutral droplets was proportional to the square root of σ/r as denoted in equation (2.2).

$$E_c^0 \propto \sigma^{1/2} r^{-1/2} \tag{2.2}$$

This critical limit has become known as the “Taylor limit of field”, or simply “Taylor limit” after Geoffrey Taylor who pioneered the corresponding theory in 1964. He refined the general relationship proposed in (2.2) to the formalized equation (2.3).

$$E_c^0 = \frac{c}{(8\pi)^{1/2}} \left(\frac{2\sigma}{\varepsilon_0 r} \right)^{1/2} \tag{2.3}$$

In equation (2.3), the empirical fitting constant c has been determined both experimentally[34-37] and theoretically,[4] and the accepted value is 1.625 for liquid droplets in air. Assuming droplets always distort into spheroidal shapes, Taylor additionally derived (2.4) and (2.5), the general relationship between an applied electric field $E < E_c^0$ and the resulting aspect ratio $\gamma = a / b$ of the major to minor axis of the spheroid.[4]

$$E = I_2 \gamma^{-4/3} \left(2 - \gamma^{-3} - \gamma^{-1} \right)^{1/2} \left(\frac{2\sigma}{\varepsilon_0 r} \right)^{1/2} \tag{2.4}$$

In equation (2.4), the coefficient I_2 is a higher-order function of γ represented by (2.5).

$$I_2 = \frac{1}{2\left(1-\gamma^{-2}\right)^{3/2}} \ln\left[\frac{1+\left(1-\gamma^{-2}\right)^{1/2}}{1-\left(1-\gamma^{-2}\right)^{1/2}} \right] - \frac{1}{1-\gamma^{-2}} \tag{2.5}$$

Equation (2.4) predicts γ increases with increasing E until $\gamma = 1.85$ where the droplet becomes unstable corresponding to $E = E_c^0$. This relationship is supported by experimental and theoretical evidence for neutral droplets and soap films in air.[35,38] Although a simple relation does not exist for $\gamma(E)$ in the spheroidal approximation, equation (2.6) approximates the relationship between γ and E in (2.4) to within 1% for fields less than 55% of the Taylor limit.[39]

$$\gamma(E) = \left(1 + \frac{9r\varepsilon_0 E^2}{16\sigma}\right)\left(1 - \frac{9r\varepsilon_0 E^2}{16\sigma}\right)^{-1} \tag{2.6}$$

Figure 2.6 and Figure 2.7 explore Taylor's spheroidal approximation as applied to droplets relevant to this thesis. Figure 2.6 shows equation (2.4) plotted for 225 μm, 500 μm, and 2.25 mm diameter droplets. Each curve demonstrates that the equilibrium aspect ratio increases with applied field for $0 < E < E_c^0$ and curves inward at higher aspect ratio values. This turning point agrees well with the Taylor limit presented by equation (2.3). At the Taylor limit, the equilibrium aspect ratio is approximately 1.85. Taylor's model was developed through a stability analysis and subsequently fails for higher field values and equilibrium aspect ratios where the droplet is no longer physically stable. Figure 2.6 demonstrates that for a given applied electric field, larger droplets will be more elliptical than smaller droplets and corroborates equation (2.3), which suggests that larger droplets require lower field strengths to become unstable and exhibit jetting.

Figure 2.7 plots the equilibrium aspect ratio for 225 μm diameter droplets of methanol and water. For a specific applied field and droplet size, droplets with a lower surface tension have a greater equilibrium aspect ratio. This plot also shows that 225 μm water droplets do not undergo jetting under standard atmospheric conditions because the necessary field is greater than the 3×10^6 V/m dielectric breakdown limit of air. For this droplet, air will break down and arc before the Taylor limit of field is reached. Indeed, inserting $E_c^0 = 3 \times 10^6$ V/m and $\sigma = 0.072$ N/m into equation (2.3), the smallest water

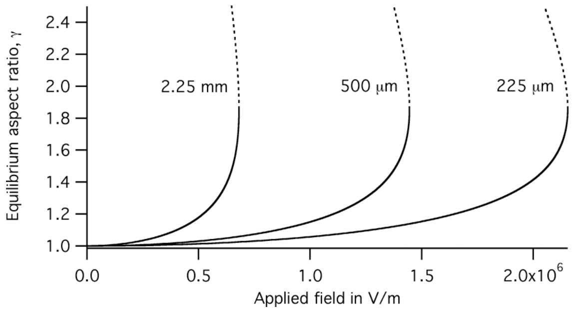

Figure 2.6. Equilibrium aspect ratio versus applied field for methanol droplets of different diameters. Solid lines are physically attainable values for the aspect ratio whereas the dotted lines represent unstable droplet shapes.

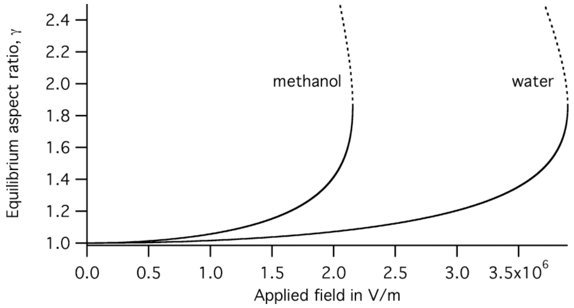

Figure 2.7. Equilibrium aspect ratio as a function of applied field for 225 μm diameter methanol and water droplets.

droplet that demonstrates jetting and FIDI would be ~380 μm in diameter. Practical considerations that lower the breakdown limit of air such as humidity and burrs on the electrodes would most likely raise the minimum water droplet diameter to about 500 μm. Between the Rayleigh limit of charge and the Taylor limit of field exists the general case where excess electrical pressure within a droplet results from both net charge and the externally applied electric field.[38,40,41] Taylor's spheroidal approximation is not as accurate at predicting shapes and critical fields because charged droplets are egg- or tear-shaped, having a higher curvature on the side carrying the net charge.[40] For a droplet of charge *q*, this shape becomes unstable at a critical electric field, E_c^q, and is characterized by the formation of a single jet from the sharper end.

2.5. Review of unresolved issues in the dynamics of charged droplets and neutral droplets in high electric fields

Research is still needed to develop a complete picture of both electrospray and field-induced droplet ionization mass spectrometry. The physical aspects of Rayleigh discharge have been well studied in the Beauchamp group as well as in the Davis, Agnes, and Leisner laboratories. However, few studies have probed the chemical aspects and implications of charged droplet phenomena. Differing ESI-MS peak heights are rationalized by surface/bulk analyte partitioning in the charged droplets formed by electrospray, but this has not be rigorously proved. Understanding the relationship between solvent and analyte partitioning between the progeny of a Rayleigh discharge and the parent would provide significant insight into the electrospray process and lead to further optimizations of the technique. The Agnes group has begun these studies by using the differential ion mobility within an electrodynamic balance to separate the progeny from the parent. These studies represent the beginning of important investigations that potentially include the characterization of how multiple chemically unique fluorphores partition between the progeny and the parent, mobility studies on multi-component droplets, and mass spectrometric characterization of the progeny relative to the parent droplets.

Similarly, our group has pioneered the use of field-induced droplet ionization as a complimentary technique for transferring analyte molecules from a droplet into a mass spectrometer for analysis. FIDI-MS promises to open new avenues to on-line mass analysis of the progress of chemical reactions within droplets, detection of trace gas-phase species, and mass sampling of a selected droplet from an assembly of multiple droplets. Future work may investigate more efficient mechanisms for directing the charged progeny into the inlet of a mass spectrometer and the subsequent analysis. Additionally, FIDI would benefit from analyses similar to those proposed for charged droplets to develop an understanding of the chemical and physical partitioning of solvent, analyte, and charge carriers between the progeny and the parent.

2.6. References

(1) ORNL Review, State of the Laboratory. vol. 29 no. 1-2 1995. http://www.ornl.gov/info/ornlreview/rev29-12/text/environ.htm (accessed June 16, 2005).

(2) Smith, J. N. Fundamental Studies of Droplet Evaporation and Discharge Dynamics in Electrospray Ionization, California Institute of Technology, 2000.

(3) Zeleny, J. *Phys. Rev.* **1917**, *10*, 1.

(4) Taylor, G. *Proc. R. Soc. London, Ser. A* **1964**, *280*, 383.

(5) Taylor, G. *Proc. R. Soc. London, Ser. A* **1966**, *291*, 159.

(6) Hines, R. L. *J. Appl. Phys.* **1966**, *37*, 2730.

(7) Tilney, R.; Peabody, H. W. *Brit. J. Appl. Phys.* **1953**, *4*, S51.

(8) Dole, M.; Mack, L. L.; Hines, R. L.; Mobley, R. C.; Ferguson, L. D.; Alice, M. B. *J. Chem. Phys.* **1968**, *49*, 2240.

(9) Yamashita, M.; Fenn, J. B. *J. Phys. Chem.* **1984**, *88*, 4451.

(10) Yamashita, M.; Fenn, J. B. *J. Phys. Chem.* **1984**, *88*, 4671.

(11) Wong, S. F.; Meng, C. K.; Fenn, J. B. *J. Phys. Chem.* **1988**, *92*, 546.

(12) Fenn, J. B.; Mann, M.; Meng, C. K.; Wong, S. F.; Whitehouse, C. M. *Science* **1989**, *246*, 64.

(13) *Electrospray Ionization Mass Spectrometry*; Cole, R. B., Ed.; John Wiley and Sons: New York, 1997.

(14) Rayleigh, L. *Philos. Mag.* **1882**, *14*, 184.

(15) Smith, J. N.; Flagan, R. C.; Beauchamp, J. L. *J. Phys. Chem. A* **2002**, *106*, 9957.

(16) Grimm, R. L.; Beauchamp, J. L. *Anal. Chem.* **2002**, *74*, 6291.

(17) Kebarle, P. *J. Mass Spectrom.* **2000**, *35*, 804.

(18) Cole, R. B. *J. Mass Spectrom.* **2000**, *35*, 763.

(19) Kebarle, P.; Peschke, M. *Analytica Chimica Acta* **2000**, *406*, 11.

(20) Lee, S. W.; Freivogel, P.; Schindler, T.; Beauchamp, J. L. *J. Am. Chem. Soc.* **1998**, *120*, 11758.

(21) Taflin, D. C.; Ward, T. L.; Davis, E. J. *Langmuir* **1989**, *5*, 376.

(22) Gomez, A.; Tang, K. *Phys. Fluids* **1994**, *6*, 404.

(23) Duft, D.; Lebius, H.; Huber, B. A.; Guet, C.; Leisner, T. *Phys. Rev. Lett.* **2002**, *89*, art. no. 084503.

(24) Li, K.-Y.; Tu, H.; Ray, A. K. *Langmuir* **2005**, *21*, 3786.

(25) Duft, D.; Atchtzehn, T.; Muller, R.; Huber, B. A.; Leisner, T. *Nature* **2003**, *421*, 6919.

(26) Feng, X.; Bogan, M. J.; Agnes, G. R. *Anal. Chem.* **2001**, *73*, 4499.

(27) Widmann, J. F.; Aardahl, C. L.; Davis, E. J. *Aerosol Science and Technology* **1997**, *27*, 636.

(28) Richardson, C. B.; Pigg, A. L.; Hightower, R. L. *Proc. Roy. Soc. A* **1989**, *422*, 319.

(29) Roulleau, M.; Desbois, M. *J. Atmos. Sci.* **1972**, *29*, 565.

(30) Schweizer, J. D.; Hanson, D. N. *J. Colloid and Interface Sci.* **1971**, *35*, 417.

(31) Berg, T. G. O.; Trainor, R. J.; Vaughan, U. *J. Atmos. Sci.* **1970**, *27*, 1173.

(32) Ataman, S.; Hanson, D. N. *Ind. Eng. Chem. Fundam.* **1969**, *8*, 833.

(33) Doyle, A.; Moffett, D. R.; Vonnegut, B. *J. Colloid Sci.* **1964**, *19*, 136.

(34) Macky, W. A. *Proc. Roy. Soc. A* **1931**, *133*, 565.

(35) Wilson, C. T. R.; Taylor, G. I. *Proc. Cambridge Philos. Soc.* **1925**, *22*, 728.

(36) Nolan, J. J. *Proc. R. Ir. Acad. Sect. A* **1926**, *37*, 28.

(37) Inculet, I. I.; Kromann, R. *IEEE Trans. Ind. Appl.* **1989**, *25*, 945.

(38) Basaran, O. A.; Scriven, L. E. *Phys. Fluids A* **1989**, *1*, 799.

(39) Saville, D. A. *Annu. Rev. Fluid Mech.* **1997**, *29*, 27.

(40) Abbas, M. A.; Latham, J. *J. Fluid Mech.* **1967**, *30*, 663.

(41) Abbas, M. A.; Latham, J. *Q. J. R. Met. Soc.* **1969**, *95*, 63.